

# INTEGRATING HUMAN AND MACHINE INTELLIGENCE IN MORPHOLOGY CLASSIFICATION TASKS WITH GALAXY ZOO EXPRESS

MELANIE BECK, AUTHOR2, AUTHOR3, ETC.

Minnesota Institute for Astrophysics, University of Minnesota, Minneapolis, MN 55454

## ABSTRACT

Quantifying galaxy morphology is a challenging yet scientifically rewarding task. As the scale of data continues to increase with upcoming surveys, traditional classifications methods will struggle to handle the load. We present a solution to the scale problem through an integration of visual and machine classifications which preserves the best features of both human and automatic classifications. We demonstrate the effectiveness of such a system through a re-analysis of visual galaxy morphology classifications collected during the Galaxy Zoo 2 project and combine these with a machine algorithm which learns on a suite of non-parametric morphology indicators widely used for automated morphologies. Our method provides an order of magnitude improvement in the rate of galaxy morphology classifications while maintaining highly accurate, pure and complete samples and requires a minimal amount of computational cost. This result has important implications for the development of galaxy morphology identification tasks in the era of Euclid and other large-scale surveys.

*Keywords:* galaxy morphology — classification — machine learning

## 1. INTRODUCTION

Astronomers have made use of galaxy morphologies to understand the dynamical structure of these systems since at least the 1930s (e.g., [Hubble 1936](#)). The division between early-type and late-type systems corresponds, for example, with a wide range of parameters from mass to environment and star formation history (e.g., [Shen et al. 2003](#); [Peng et al. 2010](#)), and detailed observation of morphological features such as bars and bulges provide information about the history of their host systems (e.g., review by [Kormendy & Kennicutt 2004](#); [Masters et al. 2011](#); [Simmons et al. 2014](#)). Modern studies of morphology divide systems into broad classes (e.g., [Conselice 2006](#); [Lintott et al. 2008](#); [Kartaltepe et al. 2015](#); [Peth et al. 2016](#)), but a wealth of information can be gained from identifying new and often rare classes, such as the green peas ([Cardamone et al. 2009](#)) and beans ([Schirmer et al. 2016](#)).

While Galaxy Zoo has provided a solution that scales visual classification for current surveys ([Willett et al. 2013, 2016](#); [Simmons et al. 2016](#)), upcoming surveys such as LSST and Euclid will require a different approach; one appropriate to tackle very large data sets. Standard visual morphology methods will be unable to contend with the scale of data, and current automated morphologies provide only statistical morphological structure with large uncertainties (e.g., [Abraham et al. 1996](#); [Bershady et al. 2000](#)).

One solution is full automation. One approach is to define a set of features which describe the morphology in an N-dimensional space. Decision boundaries within this space define morphological types for each galaxy. Learning these decision boundaries can be achieved through machine learning techniques such as support vector machines ([Huertas-Company et al. 2008](#)) or principal component analysis ([Scarlata et al. 2007](#)). Another approach is through deep learning, a machine learning technique that attempts to model high level abstractions. Algorithms like convolutional neural networks have been used with impressive accuracy ([Dieleman et al. 2015](#); [Huertas-Company et al. 2015](#)). However, a drawback to all automated classification techniques is the need for standardized training data, with more complex algorithms requiring more data. Furthermore, that data must be consistent for each survey as differences in resolution and depth can be inherently learned by the algorithm making their application to disparate surveys challenging.

In this work we seek a system which preserves the best features of both human and automatic classifications, developing for the first time a system which brings both human and machine intelligence to the task of galaxy morphology in a way that can tackle the scale and scope of next generation data. We demonstrate the effectiveness of such a system through a re-analysis of visual galaxy morphology classifications collected during the Galaxy Zoo 2 project, and combine these classifications

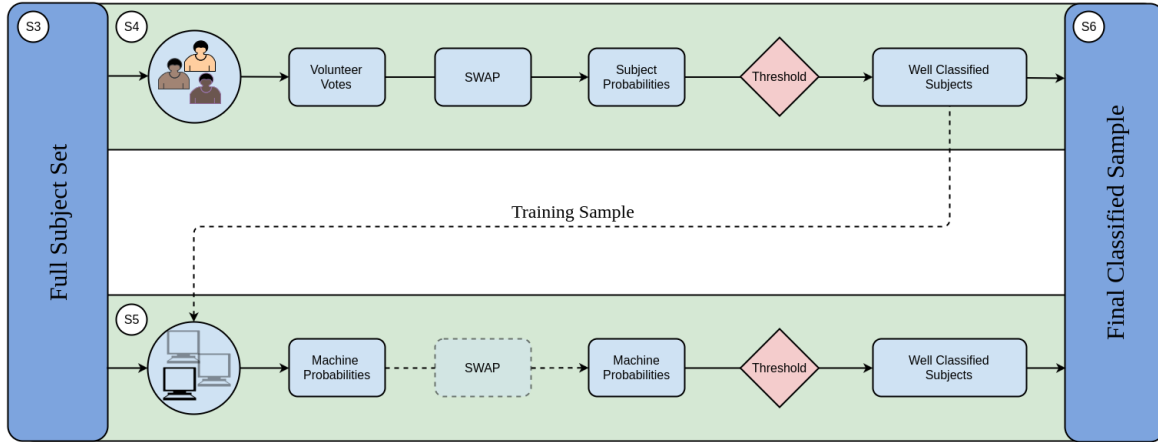


**Figure 1.** Schematic of our hybrid system. Human classifiers are shown images of galaxies via the Galaxy Zoo web interface. These classifications are recorded and processed according to section XXX. As a result of the processing, those subjects whose probabilities cross the classification thresholds are passed to the machine classifier as a training sample. The trained machine is then applied to the remaining subjects in the database (test sample). Those subjects which the machine classifies with high confidence are removed from the sample and considered fully classified. The rest remain in the database to be seen by human classifiers.

with a suite of non-parametric morphology indicators widely used for automated morphologies. Our method provides an order of magnitude improvement in the rate of galaxy morphology classifications while maintaining highly accurate, pure and complete samples.

## 2. GALAXY ZOO EXPRESS OVERVIEW

In Galaxy Zoo Express (GZX) we combine humans and machines with the goal of increasing galaxy morphology classification efficiency, both in terms of the rate of classification over time and in the amount of human effort required. Figure 1 presents a schematic of GZX which includes section numbers as a shortcut for the savvy reader. We note that transparent portions of the schematic represent areas of future work which we explore in section 7.

Any system combining human and machine classifications will have a set of generic features: a group of human classifiers, at least one machine classifier, and a decision engine which determines how these classifications should be combined.

We draw from the Galaxy Zoo 2 (GZ2) classification database which allows us to create simulations of human classifiers (described in section 3). These classifications are used most effectively when processed with SWAP, a Bayesian code described in section 4, first developed for the Space Warps gravitational lens discovery project. These subjects become the basis for the machine's training sample.

In section 5 we incorporate a machine classifier; where, for this project, we have developed a random forest classifier which trains on easily measured physical parameters relevant to galaxy morphology such as Concentration, Asymmetry, Gini coefficient and  $M_{20}$  as input. After a batch of (human) classifications is processed, the

machine is trained and its performance assessed against a validation sample. This procedure is repeated and the machine grows in accuracy as the size of the training sample increases (to a point). Once the machine reaches an acceptable level of performance it is run against the remaining galaxy sample. Images reliably classified by machine are not further classified by humans.

Even with this simple description, one can see that the classification process will progress in three phases. At first, the machine will not yet have reached the acceptable level of performance and the only subjects classified are those for which human classifiers have reached consensus. Secondly, the machine will rapidly improve and both humans and machine will be responsible for classification. Finally, improvement in the machine performance will slow and the remaining images will likely need to be classified by humans (if they can be classified at all). These results are explored in section 6. This blueprint allows even moderately successful machine learning routines to make significant contributions alongside human classifiers and removes the need for ever-increasing performance in machine classification.

## 3. GALAXY ZOO 2 CLASSIFICATION DATA

Our simulations utilize original classifications made by volunteers during the GZ2 project. These data are described in detail in Willett et al. (2013) though we provide a brief overview here. The GZ2 subject sample was designed to consist of the brightest 25% ( $r$  band magnitude  $< 17$ ) of galaxies residing in the SDSS North Galactic Cap region from Data Release 7 and included subjects with both spectroscopic and photometric redshifts out to  $z < 0.25$ . In total, 285,962 subjects were

classified in the GZ2 Main Sample catalogs<sup>1</sup>.

Subjects were shown as color composite images via a web-based interface wherein volunteers answered a series of questions pertaining to the morphology of the subject. With the exception of the first question, subsequent queries were dependent on volunteer responses from the previous task creating a complex decision tree. Using GZ2 nomenclature, a *classification* is defined as the total amount of information about a subject obtained by completing all tasks in the decision tree. A *task* represents a segment of the tree consisting of a *question* and possible *responses*. A subject is *retired* after it has achieved a sufficient amount of classification.

For the analysis in this paper we utilize the first task in the tree, ‘Is the galaxy simply smooth and rounded, with no sign of a disk?’ to which possible responses include ‘smooth’, ‘features or disk’, or ‘star or artifact’. This choice serves two purposes: 1) this question is one of only two questions in the GZ2 decision tree that is asked of every subject thus maximizing the amount of data we can work with, and 2) our analysis will assume a binary task and this question is simple enough to mold into such a form.

To force such a binary classification, we group ‘star or artifact’ responses with ‘features or disk’. Additionally, we define ‘true’ labels for each GZ2 subject to which we can compare labels assigned by Galaxy Zoo Express (GZX). Specifically, we take the majority vote fraction as the label for that subject. If the majority resided under ‘star or artifact’ or ‘feature or disk’, it was labeled as ‘Featured’; otherwise it was labeled ‘Not’. The GZ2 catalog assigns every subject three types of volunteer vote fractions: raw, weighted, and debiased. Debiased vote fractions are calculated to correct morphological classifications for redshift bias, a task that GZX is not yet built to handle. The weighted vote fractions serve to downgrade malicious volunteers and bots, a task we perform as well. However, because the mechanism for determining malicious volunteers is entirely different between GZ2 and GZX, we use labels derived from the GZ2 raw vote fractions ( $GZ2_{\text{raw}}$ ) as the closest comparison. We note that only 512 subjects in the GZ2 catalog have a majority ‘star or artifact’ vote fraction, contributing less than half a percent contamination.

In total, the data consist of over 16 million classifications from 83,943 individual volunteers. As we discuss in Section 4, the algorithm we use requires that every volunteer see a subset of subjects that are expertly identified by a member of the science team. 30,984 volunteers identified one or more of our gold standard sample

(see Section 4.1), thus we use only those classifications made by one of these “gold standard” volunteers. We note that these volunteers represent 36% of all users yet provide nearly 90% of the total Galaxy Zoo classification data, reducing the total number of classifications available for our simulated runs to approximately 14 million.

#### 4. EFFICIENCY THROUGH CLEVER HUMAN-VOTE PROCESSING

Galaxy Zoo 2 had a brute force subject retirement rule whereby each galaxy was required to achieve a threshold of approximately forty independent classifications. Once the project reached completion, inconsistent and unreliable volunteers were down-weighted as described in Willett et al. (2013). While this process reduces input from any malicious users or ‘bots’, it doesn’t reward or utilize those who are exceptionally skilled.

As a first step towards increasing classification efficiency, we ran a sequence of simulations on GZ2 classifications employing an algorithm that more intelligently manages subject retirement. This software was adapted from the Zooniverse project, Space Warps (Marshall et al. 2016), which searched for and discovered several gravitational lens candidates in the CFHT Legacy Survey (More et al. 2016). Dubbed SWAP (Space Warps Analysis Pipeline), the software predicted the probability that an image contained a gravitational lens given volunteers’ classifications and experience after being shown a training sample consisting of simulated lensing events. We provide a brief overview here.

The software assigns each volunteer an *agent* which interprets that volunteer’s classifications. Each agent assigns a 2 by 2 confusion matrix to their volunteer which encodes that volunteer’s probability of correctly identifying feature ‘A’, given that the subject actually exhibits feature  $A$ , and the probability of correctly identifying the absence of feature  $A$  given that the subject does not exhibit that feature. The agent updates these probabilities by estimating them as

$$P("X" | X, d) \approx \frac{N_{“X”}}{N_X} \quad (1)$$

where  $N_{“X”}$  is the number of classifications the volunteer labeled as type  $X$ ,  $N_X$  is the number of subjects the volunteer has seen that were actually of type  $X$ , and  $d$  represents the history of the volunteer, i.e., all subjects they have seen.

Each subject is assigned a prior probability that it exhibits feature  $A$ :  $P(A) = p_0$ . When a volunteer makes a classification  $C$ , Bayes’ Theorem is used to derive how the subject’s prior probability should be updated into a posterior:

$$P(A|C) = \frac{P(C|A)P(A)}{P(C|A)P(A) + P(C|N)P(N)} \quad (2)$$

<sup>1</sup> <https://data.galaxyzoo.org>

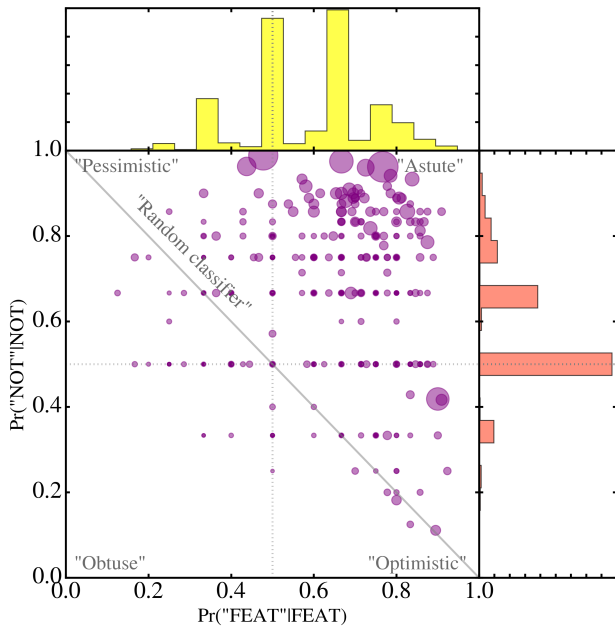


**Figure 2.** Confusion matrices for 1000 GZ2 volunteers where the size of the circle is proportional to the number of training images that volunteer classified. The distributions on the right and top represent the full sample of  $\sim 30\text{K}$  volunteers. A quarter of GZ2 volunteers are ‘Astute’ meaning that they are adept at correctly identifying both ‘Featured’ and ‘Not’ subjects. The peaks at 0.5 in both distributions are an artifact of training: a majority of volunteers see only one training image which updates only one half of their confusion matrix.

where this value can be calculated using the elements of the agent’s confusion matrix.

As the project progresses, each subject’s prior probability is continually updated, nudged to higher or lower probability depending on volunteer input. Probability thresholds can be set such that subjects crossing these thresholds are highly likely to exhibit the feature of interest or not. Subjects that cross a classification threshold are considered retired.

#### 4.1. Volunteer Training Sample

A key feature of the original Space Warps project was the training of individual volunteers through the use of simulated images. These images were interspersed with real imaging and were predominantly shown at the beginning of a volunteer’s association with the project. In this section we describe how we engineer the GZ2 data to mimic the Space Warps system as closely as possible.

We select a sample of  $\sim 3500$  SDSS galaxies for which we obtain expert classifications through the Zooniverse

platform.<sup>2</sup> These classifications were provided by approximately 15 members of the Galaxy Zoo science team. The question posed was identical to the original GZ2 question and at least five experts saw each galaxy. Votes were aggregated and a simple majority was used to provide an expert label to each of the 3500 subjects. Our final dataset consists of the classifications made by those volunteers who classify at least one of these expertly-identified galaxies. We thus retain  $\sim 14$  million classifications from  $\sim 30\text{K}$  unique volunteers. Training image classifications are processed first in all of our simulations.

Figure 2, adapted from Marshall et al. (2016), shows confusion matrices for 1000 volunteers, where the size of the circle is proportional to the number of training images that volunteer classified. The histograms represent the distribution of each component of the confusion matrix for all volunteers. Nearly 25% of volunteers are considered ‘Astute’ indicating they are generally good at correctly identifying both ‘Featured’ and ‘Not’ subjects. The spikes at 0.5 in the histograms are due to the 48% of volunteers that see only one expertly-classified training image (i.e., ‘Featured’), leaving their probability in the other (‘Not’) unchanged. Additionally, 4% of volunteers have a confusion matrix of (0.5, 0.5) indicating these volunteers classified two training images of the same type, one correctly and one incorrectly.

#### 4.2. Fiducial SWAP simulation

To simulate a live project, we run SWAP on a time step of  $\Delta t = 1$  day, during which SWAP processes all volunteer classifications with timestamps within that range. This is performed for three months of GZ2 classification data. For our fiducial simulation we start all confusion matrices at (0.5, 0.5), and set the initial subject prior probability,  $p_0 = 0.5$ . We set the ‘Featured’ threshold,  $t_F$ , i.e., the minimum probability for a subject to be retired as ‘Featured’, to 0.99. Similarly, we set the ‘Not’ threshold,  $t_N = 0.004$ . In Appendix B we explore how these initial parameters affect the SWAP output.

Because our goal is to increase the efficiency of galaxy classification, we use as a metric the cumulative number of retired subjects as a function of the original GZ2 project time. We define a subject as GZ2-retired once it achieves 30 volunteer votes since not every subject reached the 40 volunteer threshold as discussed in Willott et al. (2013). A subject is considered SWAP-retired once its posterior probability crosses either of the retirement thresholds defined above.

<sup>2</sup> The Project Builder template facility can be found at <http://www.zooniverse.org/labs>.

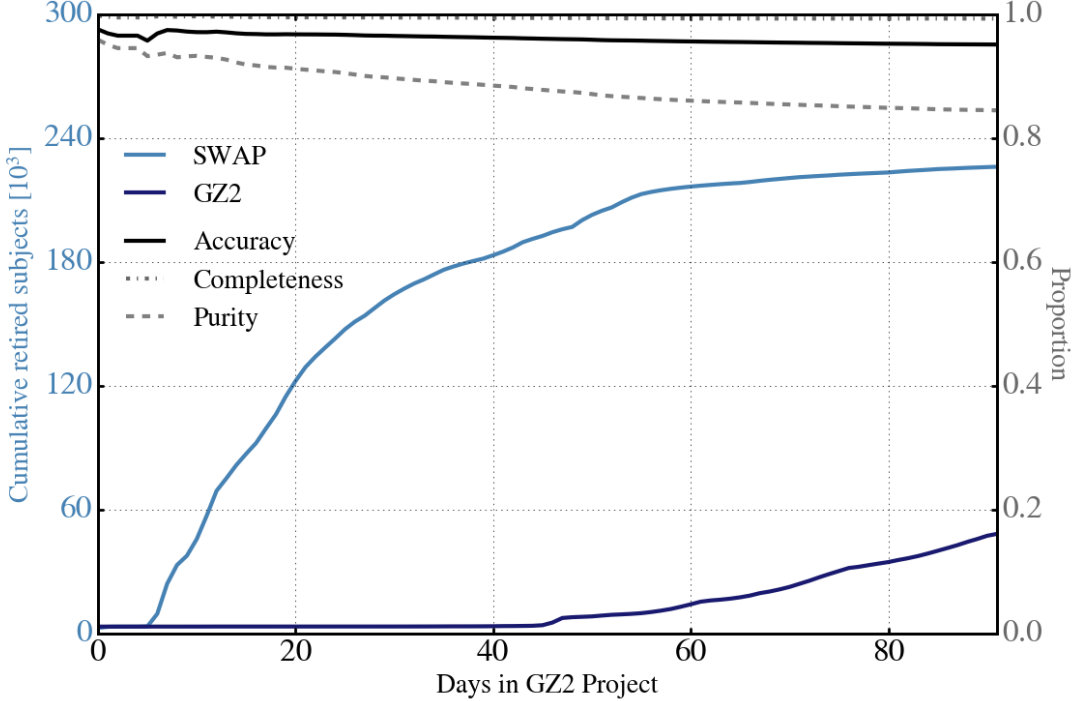


**Figure 3.** Fiducial SWAP simulation demonstrating the dramatic increase in the subject retirement rate as a function of GZ2 project time (in light blue) compared with the original GZ2 project (dark blue) corresponding to the left axis. Not only is efficiency increased by a factor of four or more, we maintain high quality classifications as shown by high marks in accuracy, completeness and purity which correspond to the right axis. Specifically, these metrics are computed on the sample obtained by that day in GZ2 project time, e.g. on day 20, these metrics are computed on the 120K subjects which SWAP has classified by that time; their SWAP labels compared to ‘true’ labels derived from published GZ2 data.

However, it is important not to prioritize efficiency at the expense of quality. We thus also consider the metrics of accuracy, purity and completeness as a function of GZ2 project time. These are defined as follows: accuracy is the number of correctly identified subjects divided by the total number retired; completeness is the number of correctly identified ‘Featured’ subjects divided by the number of actual ‘Featured’ retired; and purity is the number of correctly identified ‘Featured’ subjects divided by the number of subjects retired as ‘Featured’. Thus, a complete sample has no false negatives whereas a pure sample has no false positives.

We compute these metrics by comparing the SWAP-assigned labels of the cumulatively retired subject set to the GZ2<sub>raw</sub> labels. For example, Figure 3 shows that by Day 20, SWAP retired 120K subjects. Comparing those SWAP labels to GZ2<sub>raw</sub> labels, we find that the sample is 96% accurate, 99.7% complete, and 92% pure.

Figure 3 shows the results of our fiducial SWAP simulation compared to the original GZ2 project. The left axis shows the cumulative number of retired subjects as a function of GZ2 project time. After 90 days, GZ2 retires  $\sim$ 50K subjects while SWAP retires more than 225K. We thus classify 80% of the entire GZ2 sample in

three months. As the original GZ2 project took approximately a year to complete, this represents a factor of four increase in the rate of classification.

We also consider the reduction in human effort required to classify this subject set. Figure 4 shows the distribution of the number of volunteer classifications per subject achieved through SWAP (light blue) and GZ2 (dark blue). As expected, GZ2’s distribution peaks around  $\sim$ 45 indicating that, on average, 45 unique volunteers classify each subject. On the other hand, SWAP’s distribution peaks around 9 classifications per subject. Furthermore, subjects that are ‘easy’ to classify (i.e., ‘Featured’) require even fewer classifications to reach strong consensus. More precisely, SWAP processed a total of  $2.3 \times 10^6$  volunteer classifications while GZ2 required  $\sim 10^7$  for the same subject set. Again, this is more than a factor of four reduction in human effort.

#### 4.3. Disagreements between SWAP and GZ2

Galaxy Zoo’s strength comes from the consensus of dozens of volunteers voting on each subject. Processing votes with SWAP reduces this consensus to its bare minimum. Though we typically recover the GZ2 label, SWAP disagrees about 5% of the time. We thus exam-

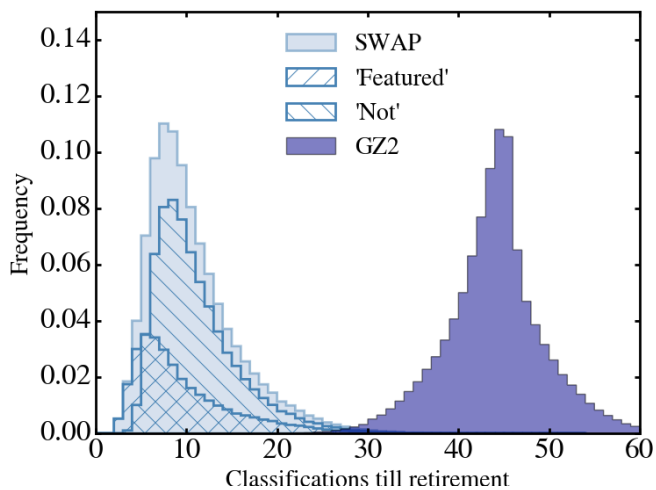


**Figure 4.** SWAP requires four times less human effort than GZ2 as evidenced by the distribution of the number of classifications a subject receives before retirement for the  $\sim 225K$  subjects retired during our fiducial run. As expected, the GZ2 distribution peaks around 45 classifications per subject. In contrast, most subjects need only 10 classifications when processing volunteer votes with SWAP.

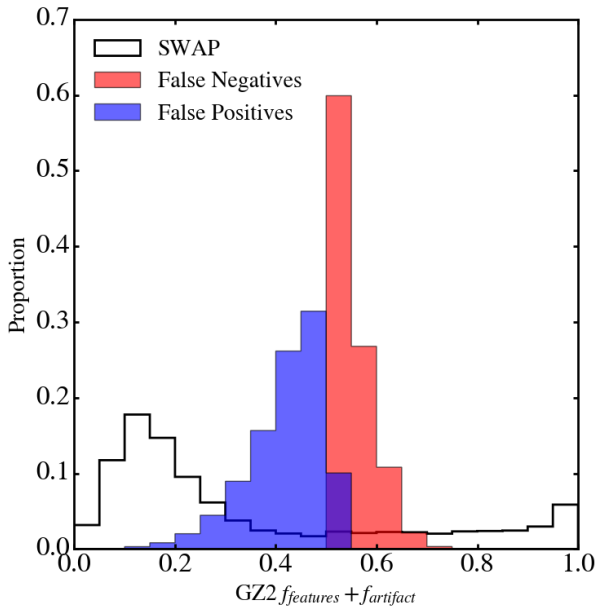


**Figure 5.** The right panel shows the distribution of GZ2 ‘features or disk’ + ‘star or artifact’ raw vote fractions for subjects identified as false positives (blue) and false negatives (red). The solid distribution represents all subjects retired by SWAP. Vote fractions between 0.4 and 0.6 indicate that volunteers were uncertain on the nature of those subjects. That SWAP doesn’t assign a matching label is not surprising.

ine the false positives, i.e., subjects which SWAP labels as ‘Featured’, but which GZ2<sub>raw</sub> labels as ‘Not’, and similarly for false negatives.

We find that the majority of these disagreements are

due to uncertainties in the GZ2<sub>raw</sub> label. Figure 5 shows the distribution of the GZ2 raw vote fraction for all subjects retired by SWAP (solid black line), the false positives (blue), and the false negatives (red). Here,  $f_{features}$  is the fraction of volunteers who classified a subject as ‘Featured’, and equivalently for  $f_{artifact}$ . A combined fraction greater than 0.5 defines a ‘Featured’ galaxy according to our GZ2<sub>raw</sub> labels. The majority of incorrectly labeled subjects have  $0.4 \leq f_{features} + f_{artifact} \leq 0.6$ , indicating that the GZ2 raw vote fractions are simply too uncertain to provide high quality labels.

Two smaller effects contribute to the disagreement between SWAP and GZ2. First, as the number of classifications used to retire a galaxy decreases, the likelihood of misclassification by random chance increases. Second, disagreement arises due to expert-level volunteers whose confusion matrices are close to 1.0. These volunteers are essentially more strongly weighted allowing that subject’s posterior to cross a retirement threshold in as few as two classifications. In some cases, these expert-level volunteers disagreed with the majority. These issues can be mitigated by requiring each subject reach a minimum number of classifications before allowing its probability to cross a threshold thus combining the best qualities of GZ2 and SWAP.

#### 4.4. Summary

We demonstrate a factor of four or more increase in classification efficiency while maintaining accuracy over 95%, nearly perfect completeness of ‘Featured’ subjects, and with a purity that can be controlled by careful selection of input parameters to be better than 90% (see Appendix B). We explore those subjects wherein SWAP and GZ2 disagree and conclude that the majority of this disagreement stems from uncertainty in GZ2<sub>raw</sub> labels. We now turn our focus towards incorporating a machine classifier utilizing these SWAP-retired subjects as a training sample.

## 5. EFFICIENCY THROUGH INCORPORATION OF MACHINE CLASSIFIERS

In this section we construct the full Galaxy Zoo Express by incorporating supervised learning, the machine learning task of inference from labeled training data. The training data consist of a set of training examples, and must include an input feature vector and a desired output label. Generally speaking, a supervised learning algorithm analyzes the training data and produces an inferred function that can then be mapped to new examples. An optimized algorithm will correctly determine class labels for unseen data. In general, most classification algorithms can handle prediction of several labels simultaneously. Work has been done to predict the en-

tirety of GZ2 classification labels using deep learning ([Dieleman et al. 2015](#)) with great success. However, it is still simpler for a machine to predict fewer labels than it is to predict several dozen, [[citation?](#)], with the additional bonus that fewer class labels require less training data. By processing human classifications through SWAP we obtain a discrete, binary task for a machine to tackle. We briefly outline the technical details of our machine classifier before turning towards the decision engine we develop for GZX in section [5.4](#).

### 5.1. Random Forests

Because our task is simple, we choose a simple machine. In particular, we use a Random Forest (RF) algorithm, an ensemble classifier that operates by bootstrapping the training data and constructing a multitude of individual decision tree algorithms, one for each subsample. An individual decision tree works by deciding which of the input features best separates the classes. It does this by performing splits on the values of the input feature that minimize the classification error. These feature splits proceed recursively. As such, decision trees alone are prone to overfitting the training data thus precluding them from generalizing well to new data. Random Forests mitigate this effect by combining the output label from a multitude of decision trees. In particular we use the `RandomForestClassifier` from the Python module `scikit-learn` ([Pedregosa et al. 2011](#)).

### 5.2. Cross-validation

Of fundamental importance is the task of choosing an algorithm’s hyperparameters, values which determine how the machine learns. In the case of a RF, these include the maximum depth of the tree, the minimum leaf size, the maximum number of leaf nodes, etc. The goal is to determine which values will optimize the machine’s performance and thus cannot be chosen *a priori*. We perform a  $k$ -fold cross-validation whereby the training sample is split into  $k$  subsamples. One subsample is withheld to estimate the machine’s performance while the remaining data is used to train the machine. This is performed  $k$  times and the average performance value is recorded. The entire process is repeated for every combination of the hyperparameter space and values that optimize the output are chosen.

### 5.3. Feature Representation and Pre-Processing

Machine learning algorithms require a feature vector for each training example. This vector is composed of  $D$  individual numeric quantities associated with the subject which the machine will use to discern that subject from others in the training sample. To segregate ‘Featured’ from ‘Not’, we draw on ZEST ([Scarlata et al. 2007](#)) and compute concentration,  $C$ , asymmetry,  $A$ ,

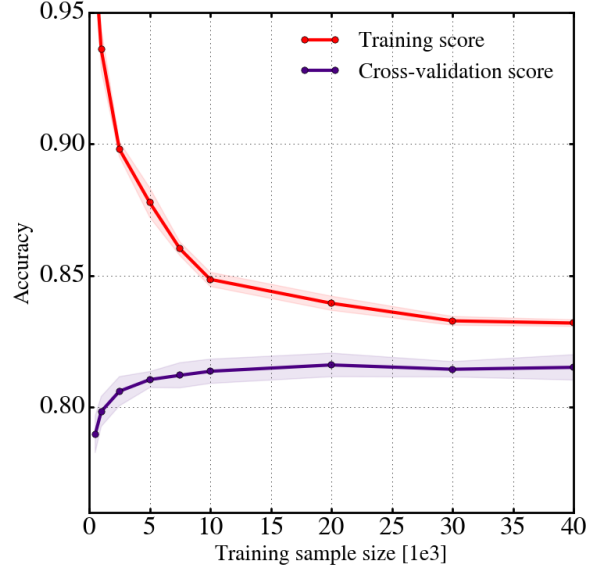


**Figure 6.** Learning curve for a Random Forest with fixed hyperparameters (maximum depth of tree, number of trees, etc.). The training score is the accuracy of the trained machine applied to its own training sample. The cross-validation score is the accuracy of the machine computed during the cross-validation process. When the training sample size is small, the machine is able to accurately identify its own training sample but is unable to generalize to unseen data, as evidenced by a low cross-validation score. As the training sample size increases, the cross-validation score increases demonstrating that the machine is more adept at generalization. This behavior plateaus indicating that larger training sample sizes provide little in additional performance.

Gini coefficient,  $G$ , and  $M_{20}$ . Coupled with SExtractor’s measurement of ellipticity ([Bertin & Arnouts 1996](#)), we provide the machine with a five dimensional morphology parameter space. (See Appendix A for details of the measurement process.) These non-parametric diagnostics have long been used to quantify galaxy morphology in an automated fashion (e.g., [Abraham et al. 1996](#); [Bershady et al. 2000](#); [Conselice et al. 2000](#); [Abraham et al. 2003](#); [Conselice 2003](#); [Lotz et al. 2004](#); [Snyder et al. 2015](#)).

One particular benefit of the RF algorithm is the flexibility with which it can accept input features. Most algorithms require that each feature dimension lie on the same scale. This is not necessary with a RF. The only preprocessing required is the removal of morphological parameters which were not well measured, i.e. catastrophic failures.

### 5.4. Decision Engine

A number of decisions must be made before attempting to train the machine. Which subjects should be designated as the training sample? When should we attempt the first training session? How do we decide when

the machine has successfully trained enough to be applied to unseen subjects? These are the core issues that we address in our machine learning decision engine.

**Which subjects should provide the training sample?** As discussed in detail in 4, SWAP yields a probability that a subject exhibits the feature of interest. A RF requires distinct classes so we use only those subjects which have crossed either of the retirement thresholds. However, subjects do not cross these thresholds with equal rates. At any given stage in the simulation, the ratio of retired ‘Featured’ to ‘Not’ is not guaranteed to be balanced which lead to sub-optimal learning. However, as a first test, we allow the machine to train on all high probability subjects.

**When should we attempt the first training session?** SWAP retires a few hundred subjects in the first days of the simulation. One could, in principle, train a machine with such a small sample, but the resulting predictions on the test sample will be exceptionally poor. Furthermore, the machine won’t know that it’s performing poorly. In practice, a much larger training size is required for the machine to learn the true parameter space. There is no hard rule for choosing this number, but a RF is a simple model so we initially require at least 10K subjects before attempting the first training session.

**When has the machine trained enough?** We assess the machine’s training by considering a learning curve, an illustration of a model’s performance with increasing sample size for fixed model hyperparameters. An example is shown in Figure 6. The cross-validation score is the accuracy resulting from k-fold cross-validation. The training score is the resulting machine applied to the training sample. When the sample size is small, the cross-validation score is low while the training score is high. This is a clear demonstration of a model over-fitting the data. As the training sample size increases, the cross-validation score increases and eventually plateaus signifying that larger training sets will yield little additional gain.

We use this general feature of any machine learning process to guide our decision making by looking for the characteristic cross-validation score plateau. At each timestep, we record the machine’s training performance, including how well it scores on the training sample (to estimate overfitting), cross-validation score, and the best hyperparameters. When the machine’s cross-validations score remains within 1% on three consecutive nights, we deem the machine’s performance acceptable.

### 5.5. The Machine Shop

We can now describe a full GZX simulation. A typical run begins with human classifications processed through SWAP for several days. During that time, humans

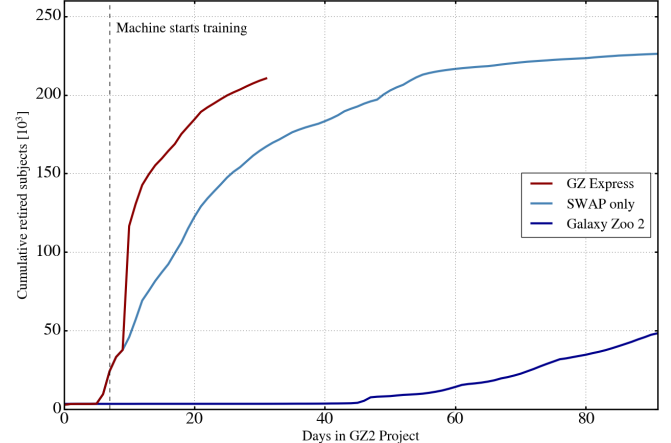


**Figure 7.** Incorporating the machine reduces the total time to classify over 200K subjects in the GZ2 sample to just 23 days. The dashed line marks when the machine trains for the first time. The machine trains for several nights before it is allowed to retire subjects. Both humans and machine then contribute to subject retirement.

‘train’ on the gold standard sample and then begin classifying the main sample. Once they retire at least 10K subjects, these are passed to the machine which trains for the first time. A suite of performance metrics are recorded by a machine agent, similar in construction to SWAP’s agents. Each night, the machine agent determines whether or not the machine has sufficiently trained by assessing all previous nights of training, comparing the variation in performance metrics. Once the machine has passed the criterion laid out above, the agent introduces the machine to the test sample which consists of any subject that has not yet been seen by humans, has not yet reached retirement through SWAP, has not been previously classified by itself, and is not part of the gold standard sample.

What constitutes a machine classification? Once the trained machine is applied to the test sample it will provide predictions for every subject therein, but these predictions are not made with the same certainty. Most machine algorithms allow one to obtain a probability associated with each subject’s predicted label. In the case of an RF, this probability is simply the average of the probabilities of each individual decision tree where the probability of a single tree is determined as the fraction of subjects of class X on a leaf node. We use this probability to assess subjects about which the machine is most confident (though we note it is not a true measure of confidence). Only subjects that receive a class prediction with  $p_{\text{machine}} \geq 0.9$  are considered retired and hence removed from the system. The remaining subjects have the possibility of being classified by humans (or the machine again) during future timesteps.

## 6. RESULTS

**Table 1.** Summary of key quantities for GZ2 and our various simulations. All quality metrics are calculated using GZ2<sub>raw</sub> labels.

Simulation Summary						
	Days	Subjects Retired	Human Effort (classifications)	Accuracy (%)	Purity (%)	Completeness (%)
Galaxy Zoo 2	430	285962	16.3 M	—	—	—
SWAP only	92	226124	2.3 M	95.7	86.7	99.0
SWAP+RF	32	210543	???	93.5	84.2	94.3

We perform a full GZX simulation incorporating both SWAP and our RF machine using the fiducial SWAP run discussed in section 4.2. The machine attempts its first training on Day 8 with an initial training sample of nearly 20K subjects. The machine undergoes several additional nights of training, each time with a larger training sample. By Day 12, the machine’s agent has assessed that the machine is suitably trained. By this point, SWAP has provided over 40K subjects as a training sample. The machine predicts class labels for the remaining 230K GZ2 subjects which are not already retired by SWAP or part of the expertly classified sample. Of those, the machine strongly predicts labels ( $p_{machine} \geq 0.9$  for nearly 71K subjects, immediately and dramatically increasing the overall sample of retired subjects. As the simulation progresses, retirement by both SWAP and the machine tapers off, though at different rates. We end the simulation after 32 days, having sufficiently classified well over 200K subjects. We present these results in the bottom panel of Figure 7 where GZX (red) is compared to our fiducial SWAP-only run (light blue) and GZ2 subject retirement (dark blue).

The top panel of Figure 7 shows our usual quality metrics for both SWAP-only and GZX, again using the GZ2<sub>raw</sub> labels discussed in section 3. Accuracy and completeness of the cumulative sample for the combined system each remain around 95% and purity remains around 85%. We note that incorporating the machine yields similar purity as when we allow SWAP to handle the entirety of the sample for a similar-sized subject set. Instead we seem to make a small sacrifice in the completeness of the ‘Featured’ sample which, in turn, affects our accuracy. Whereas SWAP alone identifies nearly all ‘Featured’ subjects it encounters, the machine appears to miss a significant portion of these thus dropping the completeness of that day’s cumulative sample. We discuss this behavior below.

By dynamically generating a training sample through a more sophisticated analysis of human classifications coupled with a machine classifier trained through a simple feedback mechanism, we are able to retire over 200K GZ2 subjects in 27 days. SWAP alone retires as many subjects in 50 days while GZ2 requires XX months to retire as many and 14 months to retire the entire cata-

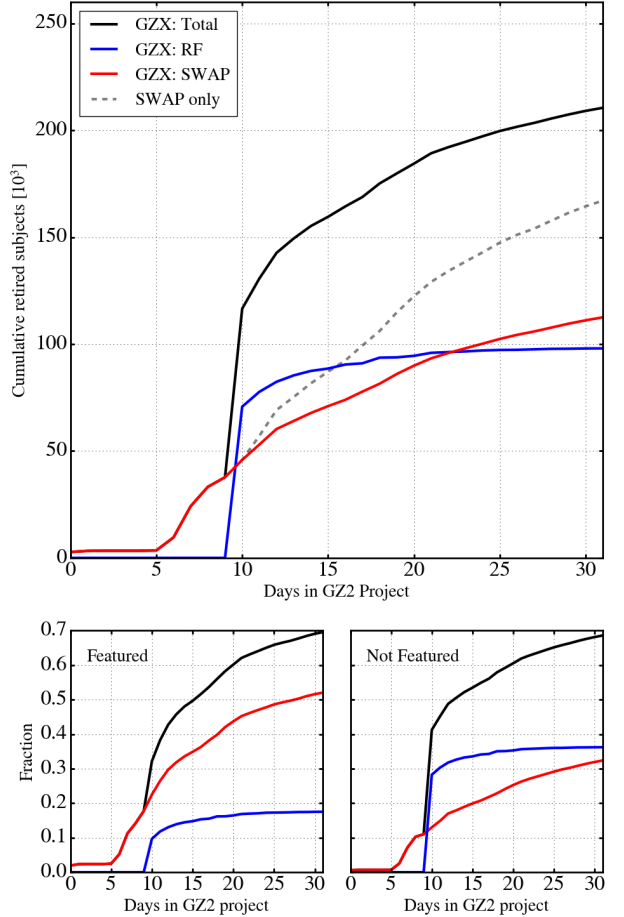


**Figure 8.** The relative contributions of the human and machine components to the number of retired subjects are nearly equal but display very different behaviors over the course of our simulation (top panel). The bottom panel shows the total fraction of subjects retired split by class label. Overall, GZX retires over 70% of the entire GZ2 sample in 32 days but the composition from each component is quite different. Humans retire more ‘Featured’ subjects than the machine and vice versa.

log of 285K subjects. GZX thus provides a full order of magnitude decrease in classification time over the traditional crowd-sourced approach. We next explore the composition of those classifications.

### 6.1. Who retires what, when?

In the top panel of Figure 8 we explore the relative contribution to subject retirement from both the ma-

chine (blue) and SWAP (red). The solid black line shows the full GZX retirement and the dashed line shows the SWAP-only fiducial run from section 4.2. Two things are immediately obvious. First, we see that, over the course of our simulation, the machine retires a total of  $\sim 100$ K subjects while SWAP retires  $\sim 110$ K subjects. Each shoulders approximately half of the classification burden. Secondly, the behavior in the rates of these retirements is clearly very different. Retirement through SWAP proceeds at a relatively constant rate. In contrast, the machine contributes a surge in retirement during its first couple days, quickly overtaking the human contribution, but plateaus thereafter. By Day 22, the human contribution through SWAP again becomes the primary mode of subject retirement.

We thus clearly see three epochs of subject retirement, as we presumed. In the first phase, humans are the only contributors to the total number of retired subjects. Once the machine has trained, it immediately contributes as much to subject retirement as humans. However, the machine’s performance plateaus faster than human performance; the third phase of subject retirement is again dominated by human classifications.

Finally, we consider the composition of the two classifying agents in the bottom panels of Figure 8. The left (right) panel shows the retired fraction of all subjects identified as ‘Featured’ (‘Not’) as a function of project time. Over the course of the simulation, SWAP retires over 50% of all ‘Featured’ galaxies in the GZ2 sample while the machine retires only 18%. Furthermore, this divergence only exists for ‘Featured’ galaxies. In the lower right panel of Figure 8, we see that both humans and machine identify similar proportions (33-37%) of the total number of ‘Not’ galaxies.

What is the source of this discrepancy? Why does the machine not identify with strong probability the remaining 30% of ‘Featured’ galaxies left unclassified by the end of our simulation? Are humans simply better at identifying featured galaxies with the machine optimized to identify the ‘Not’ subjects? Each night the machine trains, it receives a training sample that is consistently composed of 30-40% ‘Featured’ galaxies, yet a similar proportion of ‘Featured’ galaxies in the test sample do not receive high  $p_{\text{machine}}$ . Is this an artifact of our particular choice in machine, in the human-machine mechanism we’ve implemented here, or something else entirely? In the next section we explore the machine’s performance in the context of its training through human classifiers.

## 6.2. Machine performance

The analysis of the results thus far have assumed that GZ2<sub>raw</sub> labels are ground truth for every GZ2 subject. These labels were the best choice to estimate the

quality of SWAP since we were directly comparing human consensus through two different aggregation algorithms. However, the machine does not learn in the same way, nor is it presented with the same information. We argue that the machine classifications are, in fact, valid and complimentary to human classifications.

We visually examine a portion of subjects that were deemed false positives, i.e., galaxies retired as ‘Featured’ by the machine which have ‘Not’ GZ2<sub>raw</sub> labels. Figure 9 shows a random sample of images we inspected. The value in the lower left corner is the GZ2 smooth vote fraction, that is, the fraction of volunteers who classified that subject as ‘Not’. The sample consists primarily of edge-on disks and disk galaxies with low surface brightness features.

That the machine is apparently sensitive to a different information space and can identify ‘Featured’ galaxies that humans classify as ‘Not’ likely has two contributing factors: 1) the first question of the GZ2 decision tree asks a very specific question; one which doesn’t necessarily correlate with a split between early- and late-type galaxies, and 2) the machine learns on morphology diagnostics that are very different from visual inspection. Regarding the first point, we see that GZ2 smooth vote fractions are generally between 0.5 and 0.65 for this sample indicating that volunteers have not reached a strong consensus. This behavior could be modified by providing actual training images and live feedback as performed in Marshall et al. (2016). The second point suggests that the morphology indicators we measure are sufficient for the machine to recognize ‘Featured’ galaxies regardless of the labels humans provide. It remains to be seen whether this generalizes to other machine algorithms. We note that most of these galaxies are labeled as ‘Featured’ after GZ2’s debiasing process.

The complementary nature of human and machine classification can best be utilized by a feedback mechanism in which a portion of machine-retired subjects are reviewed by humans. Subjects that display excessive disagreement should be verified by an expert (or expert-user). In the same way that humans increase the machine’s training sample over time, subjects which the machine properly identifies can become part of the humans’ training sample.

## 7. LOOKING FORWARD

We have demonstrated the first practical framework for combining human and machine intelligence in galaxy morphology classifications tasks. Our results have implications for the future of citizen science in general and Galaxy Zoo in particular, however we focus instead on a brief discussion of our next steps and potential applications to large upcoming surveys.

GZX represents perhaps one of the simplest ways to

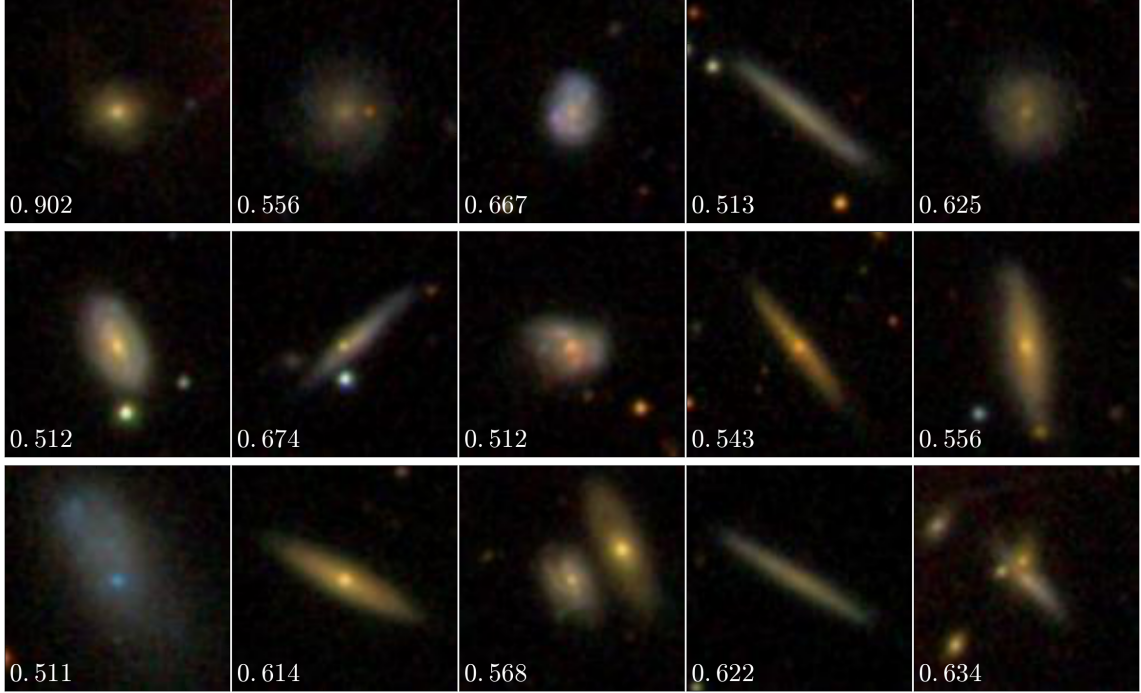


**Figure 9.** Galaxies the machine identifies as ‘Featured’ but which the majority of human classifiers labeled as ‘Not’. The number in the lower left corner is the GZ2 smooth vote fraction, that is, the fraction of volunteers who classified the subject as ‘smooth’. These values are typically between 0.5 and 0.65 indicating that humans do not reach a strong consensus.

combine human and machine intelligence. Its impressive performance motivates a higher level of sophistication. We present three of the most straightforward steps that will advance our system to the next level, implementation that will improve both the rate of quality of morphology classifications.

First, our current system contains only a passive feedback mechanism. However, we envision multiple forms of active feedback. SWAP allows us to leverage the most skilled volunteers to review those galaxies which are the most difficult for either human or machine classify. Additionally, a portion of subjects classified by machine should subsequently be reviewed by humans since we have shown that disagreements between these two agents could signify to experts that something interesting is afoot.

Secondly, the random forest algorithm is not easily adapted to handle measurement errors or class labels with continuous distributions. To fully utilize the information provided by SWAP, algorithms which can handle continuous distributions for the input and output subject labels should be explored. These include deep convolutional neural networks (CNN) or Latent Dirichlet allocation (LDA), an algorithm that is frequently used in document processing.

Finally, we envision another instance of SWAP to aggregate an ensemble of machine classifiers in a similar fashion to the human counterparts as hinted at in Fig-

ure 1. In this scheme, several disparate machine algorithms could train simultaneously on the same training sample with their predictions aggregated through SWAP.

With the above upgrades implemented, we expect performance of both the classification rate and quality to increase. However, even with our current implementation we can envision coping with the upcoming data deluge. By some estimates, Euclid is expected to obtain measurable morphology with VIS for approximately  $10^6 - 10^7$  galaxies. Traditional visual classification at the rate achieved today through Galaxy Zoo would require approximately 300 years to classify such a large dataset. GZX as currently implemented could classify the brightest 20% of the full Euclid sample within the six years of its observing mission. We predict this is a lower limit as more sophisticated machine learning algorithms will undoubtedly be capable of further efficiency.

### 7.1. Conclusions

We test a novel system for the efficient classification of galaxy morphology tasks that integrates the native ability of the human mind to identify the abstract and novel with machine learning algorithms which provide speed and brute force.

We demonstrate for the first time that the SWAP algorithm, originally developed to identify rare gravitational lenses in the Space Warps project, is robust for

use in galaxy morphology classification. We show that by implementing SWAP on GZ2 classification data we can increase the rate of classification by a factor of 4–5, requiring only 90 days of project time to sufficiently classify nearly 80% of the entire GZ2 galaxy sample.

Furthermore, we have implemented and tested a simple Random Forest algorithm and developed a decision engine that delegates tasks between human and machine. We show that even this simple machine is capable of providing significant gains in the rate of classification allowing us to retire over 70% of GZ2 galaxies in just 32 days of GZ2 project time, representing an order of magnitude increase in the classification rate compared to the original Galaxy Zoo 2 project. This is achieved without sacrificing the quality of classifications as we maintain accuracy well above 90% throughout our simulations. Additionally, we have shown that training on a 5-dimensional parameter space of traditional nonparametric morphology indicators allows the machine to

identify subjects which humans miss, providing a complementary approach to visual classification. The gain in classification speed allows us to tackle the massive amounts of data soon to be forthcoming from large surveys like LSST, Euclid, and WFIRST.

## 8. ACKNOWLEDGEMENTS

MB thanks John Wallin, Steven Bamford, and Boris Häußler for discussions which helped elucidate things and stuff.

MB, CS, LF, KW, and MG gratefully acknowledge support from the US National Science Foundation Grant AST1413610. MB acknowledges additional support through New College and Oxford University’s Balzan Fellowship as well as the University of Minnesota’s Doctoral Dissertation Fellowship. Travel funding was supplied to MB, in part, by the University of Minnesota’s Thesis Research Travel Grant. CJL recognizes support from a grant from the Science & Technology Facilities Council (ST/N003179/1).

## APPENDIX

### A. MEASURING NONPARAMETRIC MORPHOLOGICAL DIAGNOSTICS ON SDSS STAMPS

We obtain  $i$ -band imaging from SDSS data release 12. Postage stamps are made from the SDSS fields for each galaxy with dimensions of 3 Petrosian radii. Galaxies located within 3 Petrosian radii of the edge of a field were excluded. Postage stamps undergo a cleaning process whereby nearby sources are identified with SExtractor (ver. 2.8.6; [Bertin & Arnouts 1996](#)) and their pixels replaced with values that mimic the background in that region. We compute the following widely adopted nonparametric measurements of the galaxy light distribution on the cleaned postage stamps:

Concentration is computed as  $C = 5 \log(r_{80}/r_{20})$  where  $r_{80}$  and  $r_{20}$  are the radii containing 80% and 20% of the galaxy light respectively. Large values of this ratio tend to indicate disk-like galaxies, while smaller values correlate with early-type ellipticals.

Asymmetry quantifies the degree of rotational symmetry in the galaxy light distribution (not necessarily the physical shape of the galaxy as this parameter is not highly sensitive to low surface brightness features). A correction for background noise is applied (as in e.g. [Conselice et al. \(2000\)](#)), i.e.,

$$A = \frac{\sum_{x,y} |I - I_{180}|}{2 \sum |I|} - B_{180} \quad (\text{A1})$$

where  $I$  is the galaxy flux in each pixel  $(x, y)$ ,  $I_{180}$  is the image rotated by 180 degrees about the galaxy’s central pixel, and  $B_{180}$  is the average asymmetry of the background.

The Gini coefficient,  $G$ , ([Glasser 1962](#); [Abraham et al. 2003](#)) describes how uniformly distributed a galaxy’s flux is. If  $G$  is 0, the flux is distributed homogeneously among all galaxy pixels.; if  $G$  is 1, the light is contained within a single pixel. This term correlates with  $C$ , however,  $G$  does not require that the flux be in the central region of the galaxy. We follow [Lotz et al. \(2004\)](#) by first ordering the pixels by increasing flux value, and then computing

$$G = \frac{1}{|\bar{X}|n(n-1)} \sum_i^n (2i - n - 1) |X_i| \quad (\text{A2})$$

where  $n$  is the number of pixels assigned to the galaxy, and  $\bar{X}$  is the mean pixel value.

$M_{20}$  ([Lotz et al. 2004](#)) is the second order moment of the brightest 20% of the galaxy flux. We compute it as

$$M_{tot} = \sum_i^n f_i [(x_i - x_c)^2 + (y_i - y_c)^2] \quad (\text{A3})$$

$$M_{20} = \log_{10}\left(\frac{\sum_i M_i}{M_{tot}}\right), \quad \text{while } \sum_i f_i < 0.2f_{tot} \quad (\text{A4})$$

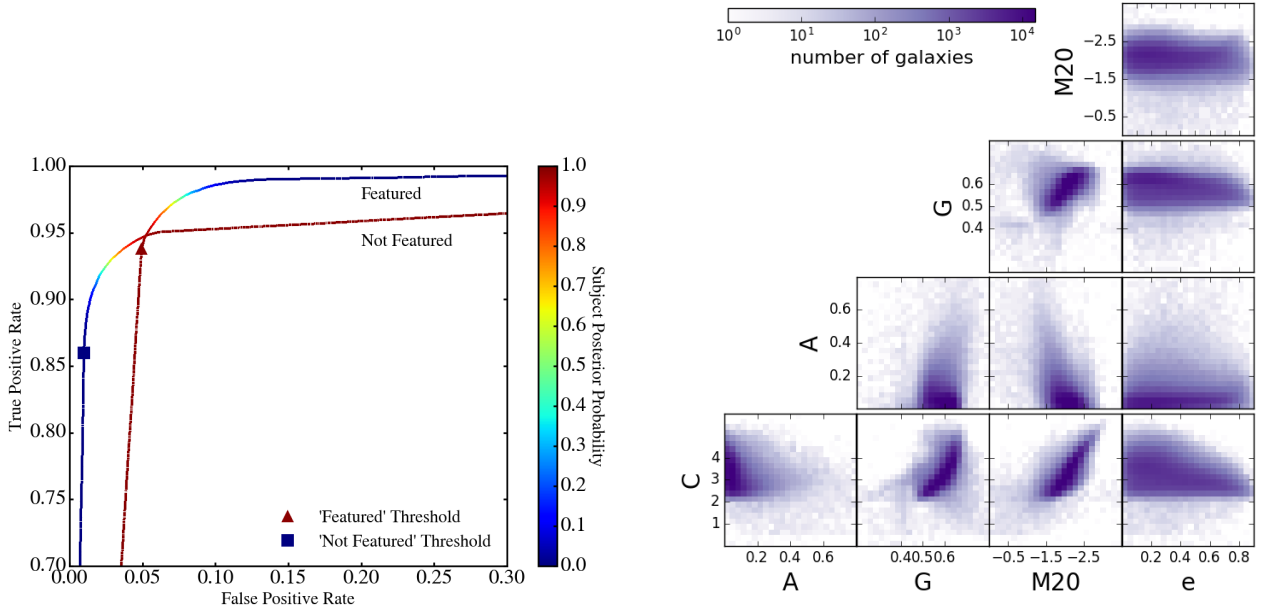


**Figure A1.** *Left.* Identifying ‘Featured’ subjects is independent of identifying ‘Not’ subjects. Both ROC curves use all subjects processed by SWAP where the score used to create the ROC curve is simply each subject’s achieved posterior probability. The Featured curve demonstrates how well we identify ‘Featured’ subjects with a threshold of 0.99, while the Not Featured curve demonstrates how well we identify ‘Not’ subjects with a threshold of 0.004. Typically, best performance is achieved with scores that lie closest to the upper left corner. Our ‘Featured’ threshold is nearly as optimal as possible though our ‘Not’ threshold could have been slightly better. *Right.* Relation between morphology diagnostics measured for more than 280K SDSS galaxies classified during the GZ2 project.

where  $M_{tot}$ , the total moment, is computed first and  $f_{tot}$  is the total flux. For centrally concentrated objects,  $M_{20}$  correlates with  $C$  but is also sensitive to bright off-center knots of light.

Finally, we use the ellipticity,  $\epsilon = 1 - b/a$ , of the light distribution as measured by SExtractor which computes the semimajor axis  $a$  and semiminor axis  $b$  from the second-order moments of the galaxy light.

In total, we measure morphological indicators for 282,350 SDSS galaxies. The relations between these diagnostics for the full sample is shown in Figure A1. The code developed to clean and compute these morphology indicators is open source and can be found at [https://github.com/melaniebeck/measure\\_morphology](https://github.com/melaniebeck/measure_morphology).

## B. EXPLORING SWAP’S PARAMETER SPACE

**Initial agent confusion matrix.** In our fiducial simulation each volunteer was assigned an agent with confusion matrix  $(P_{F,0}, P_{N,0}) = (0.5, 0.5)$ , which presumes that volunteers are no better than random classifiers. We perform two simulations wherein we allow  $(P_{F,0}, P_{N,0}) = (0.4, 0.4)$ , slightly obtuse volunteers, and  $(P_{F,0}, P_{N,0}) = (0.6, 0.6)$ , slightly astute volunteers with everything else remaining constant. Results of these simulations compared to the fiducial run are shown in Figure B2. We find that we are largely insensitive to the initial agent confusion matrix probabilities both in terms of the overall number of retired subjects and in the quality of their SWAP labels.

Predictably, when  $(P_{F,0}, P_{N,0})$  are low, we retire fewer subjects in the same time frame and more subjects when  $(P_{F,0}, P_{N,0})$  are high. This is easy to understand since it takes longer for volunteers to become strong, astute classifiers when they are initially given values denoting them as obtuse. Even with this handicap, most volunteers become astute classifiers by the end of the simulation. Overall, we retire  $\sim 225K \pm 3.5\%$  subjects as shown by the light blue spread in the bottom panel of Figure B2 where the dashed blue line denotes the fiducial run.

The top panel depicts the same quality metrics computed before where the dashed lines again denote the fiducial run. The spread is within a couple per cent for any metric. Overall we maintain accuracy around 95%, as well as completeness of 99% while maintaining purity around 84%. This spread can be due to three different effects: 1) classifying a different subset of subjects, 2) retiring subjects in a different order, and 3) subjects acquiring a different SWAP label in different simulations.

We find that SWAP is exceptionally consistent. Of all the subjects retired in these runs, we find that over 99% of

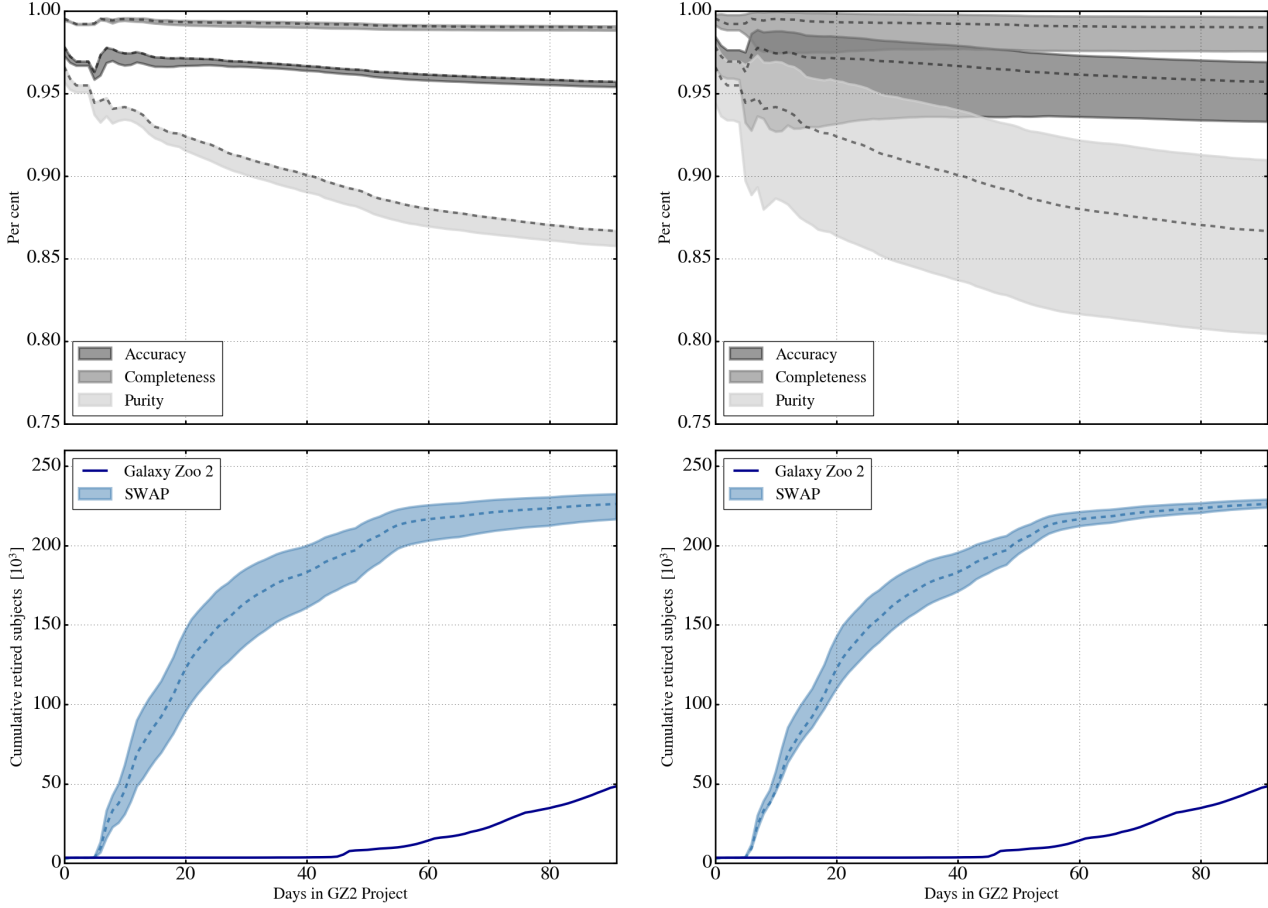


**Figure B2.** SWAP output does not dramatically change for a range of SWAP parameters. *Left.* The quality (top) and retirement rate (bottom) when different values of agent confusion matrix are assigned. *Right.* Same as the left panel but for various values of the subject prior probability. Changing the confusion matrix has little impact on the quality of the labels but varies the total number of subjects retired during the run. In contrast, changing the subject prior is more likely to affect the quality of the retirement labels rather than the total number retired.

them are the same subjects between simulations. Of those consistent between runs, we find that SWAP gives the same label for more than 99% of the subjects. What changes between runs is the order in which subjects are classified. In the low ( $P_{F,0}$ ,  $P_{N,0}$ ) run, subjects take longer to classify compared to the fiducial run (i.e., they retire on a later date in GZ2 project time). Subjects in the high ( $P_{F,0}$ ,  $P_{N,0}$ ) run retire earlier in GZ2 project time. This can cause a variation in accuracy, completeness or purity because these values are calculated on a day to day basis; if we're working with a slightly different make-up of subjects on a given day, we can expect to compute different values for these metrics. These effects each contribute less than one per cent variation and thus we see a high level of consistency between these simulations.

**Subject prior probability,  $p_0$ .** The prior probability assigned to each subject is an educated guess of the frequency of that characteristic in the scope of the data at hand. For galaxy morphologies, this number should be an estimate of the probability of observing a desired feature (bar, disk, ring, etc.). In our case, we desire to simply find galaxies that are ‘Featured’, however, this is dependent on mass, redshift, physical size, etc. The original GZ2 sample was selected primarily on magnitude and redshift. As there was no cut on the galaxy size (with the exception that each galaxy be larger than the SDSS PSF), the sample includes a large range of galaxy masses and sizes. Thus, designating a single prior is not clear-cut. We thus explore how various  $p_0$  affect the SWAP outcome.

We run several simulations where  $p_0$  is allowed to take values 0.2, 0.35, and 0.8 and compare these to the fiducial run where  $p_0 = 0.5$ , everything else remaining constant. The results are shown in Figure ??, where again we find that SWAP is consistent in terms of the total number of subjects retired during the simulation which varies by only 1%. However, as can be seen in the top panel, the variation in our quality metrics is more pronounced and deserves some

discussion.

Firstly, though we are retiring nearly the same number of subjects over the course of each simulation, they are less consistent than our previous simulations. That is, only 95% of the subjects are common to all runs. Secondly, of those that are common, only 94% receive the same label from SWAP. Changing the prior is more likely to produce a different label for a given subject than changing the initial agent confusion matrix. Finally, there is also a larger spread in the day on which a subject is retired when compared to the fiducial run, being nearly equally likely to retire ‘late’ or ‘early’ regardless of  $p_0$ . These trends all contribute to a broader spread in accuracy, completeness, and purity as a function of project time. We stress, however, that though more substantial than the previous comparison, these variations are all within  $\pm 5\%$ .

We can get a handle on these variations more intuitively by considering the following. Recall that our retirement thresholds,  $t_F$  and  $t_N$ , have not changed in these simulations. Thus when  $p_0$  is small, the subject probability is already closer to  $t_N$ , and more subjects are classified as ‘Not’ compared to the fiducial run. Similarly, when  $p_0$  is large, some of these same subjects can instead be classified as ‘Featured’ because the prior probability is already closer to  $t_F$ . Obviously, both outcomes cannot be correct and we find that the simulation with  $p_0 = 0.8$  performs the worst of any run which is a direct reflection of the fact that this prior is not suitable for this question nor for this dataset. For the mass, size, and redshift range of subjects in GZ2, we would not expect that 80% of them are ‘Featured’. Indeed, the best performance is achieved when  $p_0 = 0.35$ . This reflects the actual distribution of ‘Featured’ subjects in the GZ2 sample as well as being similar to the expected proportion of ‘Featured’ galaxies in the local universe, depending on your definition. Thus, the take-away here is to choose your prior wisely since a value far from the correct value can have a significant impact on the quality of your classifications.

**Retirement thresholds.** Retirement thresholds are directly related to the time that a subject will spend in SWAP before retiring. If we lower  $t_F$  (and/or raise  $t_N$ ), more subjects will be retired compared to the fiducial run as each subject will have a smaller swath of probability space in which to bounce back and forth before crossing one of these thresholds. On the other hand, if we raise  $t_F$  (and/or lower  $t_N$ ), it will take longer for subjects to cross one of these thresholds. Additionally, this will also increase the likelihood of some subjects never crossing either threshold as there are always some which are nudged back and forth indefinitely through probability space.

What thresholds should one choose? To answer this question, we consider Figure A1 which depicts the receiver operating characteristic (ROC) curve for our fiducial simulation. The solid line shows the curve when considering the ‘Featured’ threshold while the dotted line corresponds to ‘Not’. The square and triangle represent our thresholds,  $(t_F, t_N) = (0.99, 0.004)$ , on that curve at the end of the simulation. We see that  $t_F$  is nearly optimal but  $t_N$  could be improved upon.

Throughout this discussion we have computed quality metrics under the assumption that the ‘true’ labels provided by GZ2 are accurate. This is unlikely to be the case for every subject as Willett et al. (2013) explicitly caution against using the majority volunteer vote fraction as label since some of these are highly uncertain. We now turn to a brief discussion of those subjects where SWAP and GZ2 do not agree.

## REFERENCES

- Abraham, R. G., Tanvir, N. R., Santiago, B. X., et al. 1996, MNRAS, 279, L47
- Abraham, R. G., van den Bergh, S., & Nair, P. 2003, ApJ, 588, 218
- Bershady, M. A., Jangren, A., & Conselice, C. J. 2000, AJ, 119, 2645
- Bertin, E., & Arnouts, S. 1996, A&AS, 117, 393
- Cardamone, C., Schawinski, K., Sarzi, M., et al. 2009, MNRAS, 399, 1191
- Conselice, C. J. 2003, ApJS, 147, 1
- . 2006, MNRAS, 373, 1389
- Conselice, C. J., Bershady, M. A., & Jangren, A. 2000, ApJ, 529, 886
- Dieleman, S., Willett, K. W., & Dambre, J. 2015, MNRAS, 450, 1441
- Glasser, G. J. 1962, Journal of the American Statistical Association, 57, 648
- Hubble, E. P. 1936
- Huertas-Company, M., Rouan, D., Tasca, L., Soucail, G., & Le Fèvre, O. 2008, A&A, 478, 971
- Huertas-Company, M., Gravet, R., Cabrera-Vives, G., et al. 2015, ApJS, 221, 8
- Kartaltepe, J. S., Mozena, M., Kocevski, D., et al. 2015, ApJS, 221, 11
- Kormendy, J., & Kennicutt, Jr., R. C. 2004, ARA&A, 42, 603
- Lintott, C. J., Schawinski, K., Slosar, A., et al. 2008, MNRAS, 389, 1179
- Lotz, J. M., Primack, J., & Madau, P. 2004, AJ, 128, 163
- Marshall, P. J., Verma, A., More, A., et al. 2016, MNRAS, 455, 1171
- Masters, K. L., Nichol, R. C., Hoyle, B., et al. 2011, MNRAS, 411, 2026
- More, A., Verma, A., Marshall, P. J., et al. 2016, MNRAS, 455, 1191
- Pedregosa, F., Varoquaux, G., Gramfort, A., et al. 2011, Journal of Machine Learning Research, 12, 2825
- Peng, Y.-j., Lilly, S. J., Kovač, K., et al. 2010, ApJ, 721, 193

- Peth, M. A., Lotz, J. M., Freeman, P. E., et al. 2016, MNRAS, 458, 963
- Scarlata, C., Carollo, C. M., Lilly, S., et al. 2007, ApJS, 172, 406
- Schirmer, M., Malhotra, S., Levenson, N. A., et al. 2016, MNRAS, 463, 1554
- Shen, S., Mo, H. J., White, S. D. M., et al. 2003, MNRAS, 343, 978
- Simmons, B. D., Melvin, T., Lintott, C., et al. 2014, MNRAS, 445, 3466
- Simmons, B. D., Lintott, C., Willett, K. W., et al. 2016, ArXiv e-prints, arXiv:1610.03070
- Snyder, G. F., Torrey, P., Lotz, J. M., et al. 2015, MNRAS, 454, 1886
- Willett, K. W., Lintott, C. J., Bamford, S. P., et al. 2013, MNRAS, 435, 2835
- Willett, K. W., Galloway, M. A., Bamford, S. P., et al. 2016, ArXiv e-prints, arXiv:1610.03068